Fuel Processing Technology 277 (2025) 108308

Contents lists available at ScienceDirect

Fuel Processing Technology

journal homepage: www.elsevier.com/locate/fuproc

Investigation of the spray formation of solketal under diesel engine conditions and the influence on Diesel R33.

Julian Türck [a,b,*], Sebastian Riess [c], Lukas Strauß [c], Fabian Schmitt [b], Ralf Türck [b,d], Wolfgang Ruck [a], Michael Wensing [c,d], Jürgen Krahl [d,e]

[a] Leuphana Universität Lüneburg, Universitätsallee 1, 21335 Lüneburg, Germany
[b] Tecosol GmbH, Jahnstraße 2, 97199 Ochsenfurt, Germany
[c] FAU Erlangen-Nürnberg, Cauerstraße 4, 91058 Erlangen, Germany
[d] Fuels Joint Research Group, www.fuels-jrg.de, Germany
[e] OWL University of Applied Sciences and Arts, Campusallee 12, 32657 Lemgo, Germany

ARTICLE INFO

Keywords:
Defossilization
Spray formation
Solketal
Mass flow
Penetration depth
Drop-in capability

ABSTRACT

The defossilization of diesel fuels presents a multitude of new opportunities and challenges. Due to the increase in complexity and interactions between the components, it is necessary to examine the drop-in capability of new fuel components. One aspect of this is the influence on spray formation of the fuel. This work addresses the spray behavior of isopropylideneglycerine (solketal) and its influence on a multicomponent diesel blend (Diesel R33: 33 % renewable share). In general, it represents the first spray study of solketal. It enables value to be added from glycerin and, according to initial combustion tests, has a promising emissions profile due to its higher molecular oxygen density. The mass flow rate, penetration depth and cone angle were examined by using high-temperature and -pressure injection chamber equipped by optical diagnostics (Mie scattering setup and schlieren imaging system). These parameters are examined under varying fuel temperatures, injection pressures and ambient conditions. Solketal as a pure compound exhibits the expected behavior i.e. it is drop-in compatible even with varying parameters. The influence of solketal on Diesel R33 reveals that, in comparison to solketal-free blends, larger maximum mass flows are generated. It also shows that the penetration depths decrease (up to 34 %). In addition, there is more fuel in the gas phase, which may be a result of the comparatively low boiling point. In general, the influence of solketal suggests that fuel-induced soot reduction could be possible in existing fleets.

1. Introduction

One of the greatest challenges of modern global society is the energy transition towards sustainable technologies. However, it is imperative to investigate the extent to which these challenges can be overcome using existing technologies. Internal combustion engines (ICE) can be a factor, since a significant number of existing vehicles will remain on the market during this transition period. Therefore, the use of fuels is a crucial parameter for the short-term reduction of emissions. The emphasis in this regard is on the defossilization of fuels.

The first step in this direction was the introduction of the Diesel R33, which is composed of 26 % hydrotreated vegetable oils (HVO) and 7 % biodiesel [1]. In general, fuels are subject to technical restrictions and must be applicable in ICE. This is referred to as drop-in capability. The drop-in capability can then be distinguished between fuel properties as well as engine compatibility. The fuel drop-in capability is described by the current fuel standards (e.g. diesel fuel standard EN 590) [2]. The limit for adding HVO is due to the fact that HVO reduces density to such an extent that the overall density of the fuel blend is outside the density window of the EN 590 standard [3]. With regard to material compatibility, questions regarding the material resistance of the fuel filter [4], the seals [5] and the water separator [6] must be clarified.

Another aspect of engine drop-in capability lies in the injection process [7]. Again, HVO reduces viscosity [8], which affects atomization

Abbreviations: Θ, Cone Angle; ECN, Engine Combustion Network; EN 590, European Diesel Standard; HDA, Injection Rate Measurement; HVO, Hydrotreated Vegetable Oil; ICE, Internal Combustion Engine; LED, Light-Emitting Diode; OME, Polyoxymethylenether; p_a, Ambient Pressure; R33, Renewable share of 33 %; S, Penetration Depth; T_a, Ambien Temperature; wt%, Weight Percent.

* Corresponding author at: Leuphana Universität Lüneburg, Universitätsallee 1, 21335 Lüneburg, Germany.
E-mail address: julian.tuerck@stud.leuphana.de (J. Türck).

https://doi.org/10.1016/j.fuproc.2025.108308
Received 17 July 2025; Received in revised form 31 July 2025; Accepted 6 August 2025
Available online 14 August 2025

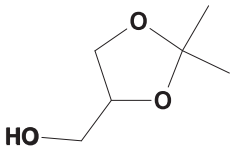

Fig. 1. Chemical structure of solketal.

and spray formation [9]. Since defossilization increases the share of HVO, a candidate should be found that acts as a counterpart in terms of density and viscosity. Therefore, glycerin has come into focus in the search for renewable resources to address this issue. In general, glycerin is a by-product of biodiesel production [10]. Glycerin from biodiesel waste plants is challenging to access the higher economic valued markets due to technical and economic reasons [11,12]. Therefore, conversion to a fuel additive may be a way to add value to glycerin. Due to the toxic emission of acrolein [13], the low calorific value [14] and further technical difficulties (insolubility in hydrocarbon [15] glycerin is not feasible as a fuel component. To overcome these limitations, chemical derivatization of glycerol is required. One promising way to convert glycerin is turn into solketal [16]. The chemical structure of solketal is shown in Fig. 1.

As a glycerin derivative, solketal has a comparatively higher molecular oxygen density compared to diesel fuel components. The increase in molecular oxygen density is caused by the two functional groups, the hydroxyl and ketal groups. In addition to overcome the technical limitations of glycerin through solketal, molecules with high molecular oxygen density are desirable as fuel components, as studies with OME have shown. These molecules tend to show less soot formation [17]. In particular, fuel research shows that solketal has a positive influence on fuel aging [18] [19] [20]. Studies on combustion behavior revealed that it has similar properties as ethanol [21]. This highlights the ignition behavior of diesel fuels containing solketal, since solketal reduces the cetane number [22]. With regard to diesel fuel testing, solketal had demonstrated that engine performance and harmful emissions have been reduced [23] and that nanoemulsions lead to good combustion efficiency [24]. Thus, solketal can influence spray formation, ignition delay and consequently emission behavior of the fuel.

In general, efficient spray formation is an essential factor in ensuring that the combustion process in the engine is as effective and low-emission as possible. The aim is to atomize the fuel, create a turbulent flow and achieve an improved air-fuel ratio. This implies that the droplets are atomized so finely that they are thin enough to mix well with the air. One way to achieve this is through the technical design of the injectors [25] and the geometry of the combustion chamber [26], as well as the injection strategy [27] and the injection pressures [28]. However, the fuel also affects the spray process and the associated atomization of its droplets. Furthermore, the fuels can influence the gas-liquid phase relationship depending on their evaporation behavior [29]. As a result, the fuels can affect the combustion temperature, e.g. through the evaporation enthalpy, which has a direct influence on the emission behavior [30,31]. Another physical parameter which is affected by fuels is the viscosity and density [32]. The change can be observed by the change in mass flow [33]. In addition, the surface tension can be influenced, which has a major impact on the size of the fuel droplets. [34].

1.1. Objective

The aim of this work is to evaluate the injection, the spray behavior of solketal and its impact on Diesel R33 fuel. Since Diesel R33 is the market-established drop-in fuel with the highest share of renewable fuels, Diesel R33 is therefore specified as the fuel matrix. The focus is on the injection rate, the depth of penetration and the cone angle using Mie and Schlieren detection.

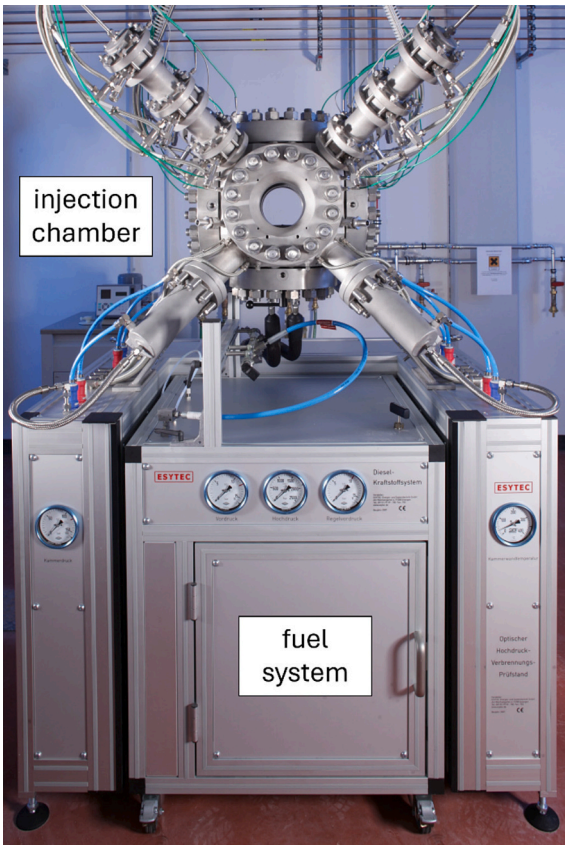

Fig. 2. High-temperature and high-pressure injection chamber with fuel supply system.

2. Experimental section

Information on the chemicals and fuels used, as well as the associated fuel analyses, is provided in the supporting information.

2.1. Injection rate measurement

A Moehwald HDA-500 injection rate measuring device is used to measure the injection rates for different fuels, injection pressures and ambient conditions. This commercially available device works on the principle of hydraulic pressure increase in a closed volume and records injection rates and injected mass with high temporal resolution [35,36]. The device reaches a mass measuring accuracy and repeatability of 0.075 mg per injection. For all injection rate experiments, the back pressure in the closed volume is 60 bar. Measurements were performed at fuel temperatures of −1, 25, and 90 °C as well as injection pressures of 500, 1000, and 1500 bar.

2.2. Test bench

The optical investigations are carried out in a high-temperature and high-pressure injection chamber (see Fig. 2). The cubic chamber body is continuously flushed with nitrogen for the presented experiments. At the four upper corners of the vessel, electric heaters increase the gas temperature in three successive stages so that up to 1000 K can be reached in the area relevant for injection processes. A combination of purge gas mass flow and a needle valve in the test bench's exhaust line allows an ambient pressure of up to 10 MPa to be generated. A research fuel injection system with two Maximator pressure amplifiers delivers an injection pressure of up to 400 MPa with low fluctuations. Five sides of the container are equipped with window flanges with visually accessible

Table 1
Operating conditions for the optical investigations.

Ambient pressure [bar]	Ambient temperature [°C]	Ambient density [kg/m^3]	Injection pressure [bar]	Fuel temperature [°C]
59	577	22.8	1500	90
62	627	22.8	500	90
62	627	22.8	1000	90
62	627	22.8	1500	90
62	627	22.8	1500	−20
62	627	22.8	1500	25
62	627	22.8	1500	90
66	677	22.8	1500	90

windows of 125 mm in accessible diameter. The bottom flange contains an injector housing for mounting the injector and for conditioning the fuel and injector temperature between −20 and 100 °C via a thermostat. The injection chamber and the fuel supply system are designed and built in-house at FAU Erlangen-Nuremberg, comply with the applicable regulations for pressure vessel and high-pressure fluid system construction, and are controlled remotely via a PLC system.

Since the vessel is constantly flushed, the ambient pressure remains constant throughout the injection process. The ambient gas flow can be considered steady compared to the velocities characteristic of injections under diesel engine conditions. Residual fuel is removed with ambient gas, which enables injection investigations at a frequency of 1 Hz. Further details can be found in Riess et al. [37].

2.3. Optical setup

A Mie scattering setup is used in the injection chamber to visualize the liquid spray. Three white light LED arrays are mounted on two side windows and the top window (not shown in schematic) of the vessel. During an injection, the light is scattered at liquid surfaces and captured by a camera system.

The gas jet is examined using a Schlieren imaging system. The light from a green LED array is collected by a lens system, parallelized and directed through the vessel normally to one spray cone. On the other side of the chamber, the light is focused and adjusted to the size of the camera lens. An image of the injected jet is captured based on the refraction of the parallelized light at optical inhomogeneities such as temperature or fuel-related density gradients.

For both measurement techniques, a Photron Fastcam SA-Z with a frame rate of 50,000 fps is used. The imaging system for the optical methods is calibrated by taking an image of a reference scale with precisely known dimensions. Considering the spatial pixel resolution of the acquired images, an uncertainty of ±0.07 mm is reached for both optical techniques. Further details on the optical measurement methods can be found in Riess et al. [37].

Table 2
List of maximum mass flows at different injection pressures and fuel temperatures. In addition, the increase in maximum mass flow when the parameters are increased was calculated and displayed.

Injection pressure [bar]	Maximum mass flow [g/s]	Increase [%]
500	8.56	–
1000	12.40	31
1500	15.09	17.8

Fuel temperature [°C]	Maximum mass flow [g/s]	Increase [%]
−1	12.49	–
25	14.58	14.3
90	15.09	3.3

For each measurement point at all test conditions, 32 injection processes are recorded to enable a statistically significant evaluation. Among other things, the cone angle and penetration depth are evaluated for both measurement methods based on a MATLAB algorithm. Definitions for penetration depth and cone as well as further details on the image evaluation can be found in Riess et al [37].

2.4. Injector and fuels

The injector used for all experiments has the body of a commercially available, piezo-controlled servo-hydraulic common rail injector, which is equipped with a special research nozzle that has three symmetrically arranged nozzle holes at an elevation angle of 45°. This allows the isolated observation of a single fuel jet. The hole diameter is 115 µm with a length-to-diameter ratio of 6.5 and a conicity factor of 2. The energizing time for the presented experiments is 1.5 ms.

Diesel R33 (67 % fossil Diesel, 26 % HVO, 7 % RME), neat solketal and blends of R33 with 3, 6 and 9 wt.-% of solketal are investigated in all experiments. In some cases, pure fossil reference Diesel fuel without any bio-content is also used for comparison.

2.5. Test conditions

The test conditions are based on the Spray A operating point of the Engine Combustion Network (ECN) and include parameter variations of injection pressure, ambient pressure and temperature, and fuel temperature as represented in Table 1.

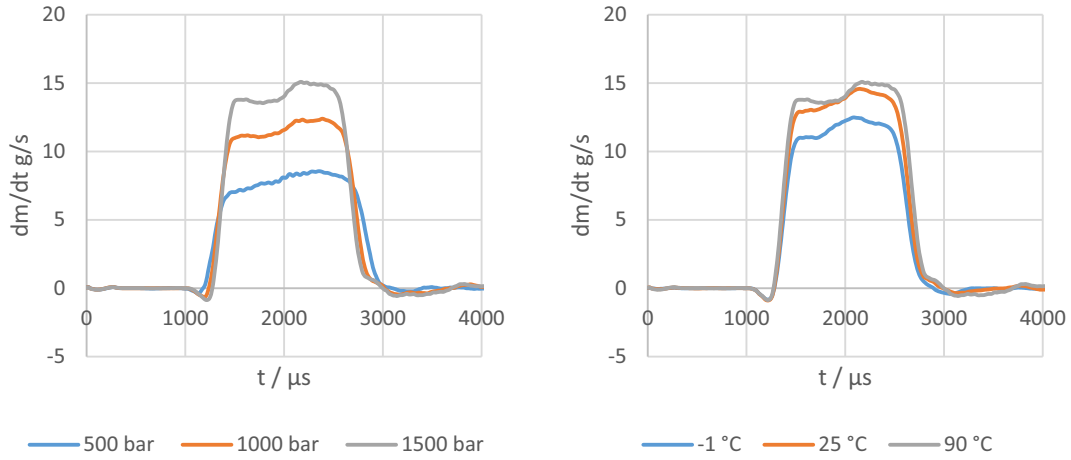

Fig. 3. HDA Measurements of neat solketal at different conditions. Left: Variation of injection pressure. Right: Variation of fuel temperature. During the measurement, the ambient pressure (60 bar) and the energizing time (1500 µs) were kept constant.

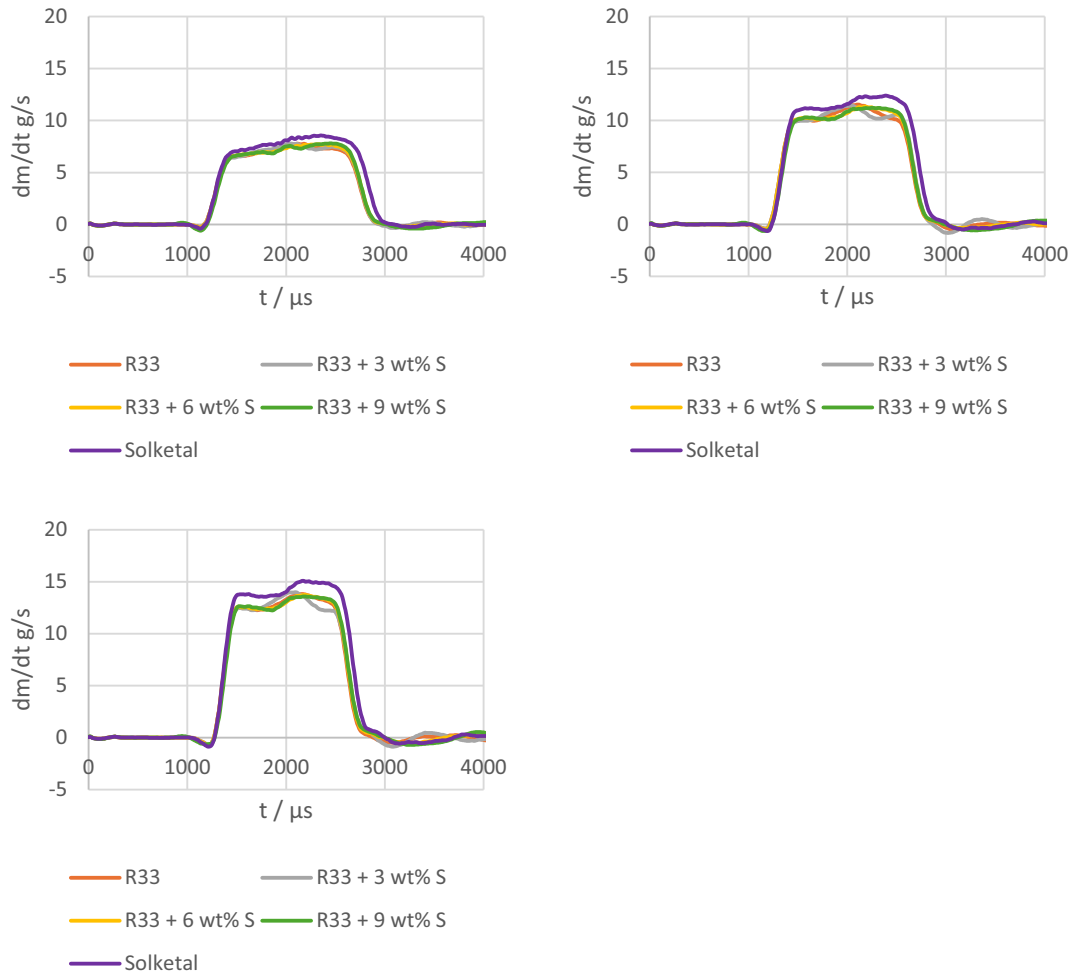

Fig. 4. Comparison of R33 pure and blended with solketal with pure solketal at different injection pressures (Top left: 500 bar, top right: 1000 bar and bottom left: 1500 bar). During the measurement, the ambient pressure (60 bar), the fuel temperature (90 °C) and the energizing time (1500 µs) were kept constant.

3. Results and discussion

3.1. Injection rate measurements (HDA)

Initially, the mass flow of pure solketal was examined at different injection pressures and fuel temperatures (see Fig. 3). It shows that an increase in injection pressure and fuel temperature results in a higher maximum mass flow rate. By comparison, the variation in injection pressure has a greater influence on the injection rate than the fuel temperature. The progressions for different physical conditions lie in different size ranges and do not overlap. In addition, the progress of mass flow rate can enable a semi-quantitative comparison. This is achieved by comparing the maximum mass flow which is measured. The determined maximum mass flows are listed in Table 2. This approach confirms the observation that the injection pressure has a stronger influence (31 and 17.8 % vs. 14.3 and 3.3 %). Accordingly, the influence of solketal on the mass flow of a multi-component diesel fuel was investigated. Fig. 4 describes the change in injection pressure and Fig. 5 the change in fuel temperature.

Due to overlaps, the comparison of maximum mass flow rates was not considered. However, qualitative comparisons can be made. Compared to pure solketal, all Diesel R33 blends show a decrease in the mass flow. Solketal has an increased density compared to other fuels and a dynamic viscosity in the range of 11 mPa per second [38]. These increased parameters enable solketal to achieve a higher injection rate compared to the Diesel R33 blends. The overall densities are listed in Table 3. Only slight differences were found in the injection pressure compared to the Diesel R33 blends. The comparatively larger influence is seen in the variation of the injection pressure itself.

When the fuel temperature is varied, it is confirmed that pure solketal has the highest injection rate. The variation in the ranges of the rates is lower compared to that of the different injection pressures. Again, only very minor influences of solketal on the overall mixtures of Diesel R33 can be assumed. The fact that the injection rates for Diesel R33 are in a similar range should be due to the fact that solketal was added in small quantities. Regardless of this, it is shown that the mass flow is of the same order of magnitude as established fuels such as Diesel R33, which supports a drop-in capability in the injection systems of existing fleets. However, further parameters such as material compatibility must be taken into account in order to confirm complete drop-in compatibility.

3.2. Spray investigation of pure solketal

Before the influence of solketal as a diesel component can be evaluated, the spray behavior of neat solketal under diesel engine conditions should be investigated first. The values and progressions for penetration depths and cone angles discussed below can be found in Figs. 6–7 and Tables 4–5. The fuel temperature before injection, the injection pressures and the ambient conditions are varied, and the penetration depth of the fuel is examined with simultaneous determination of the cone angle. The observations are carried out in both the liquid and gas phases. During the spread of the spray, the penetration depth in the liquid phase approaches an approximately constant value. In the gas phase, however,

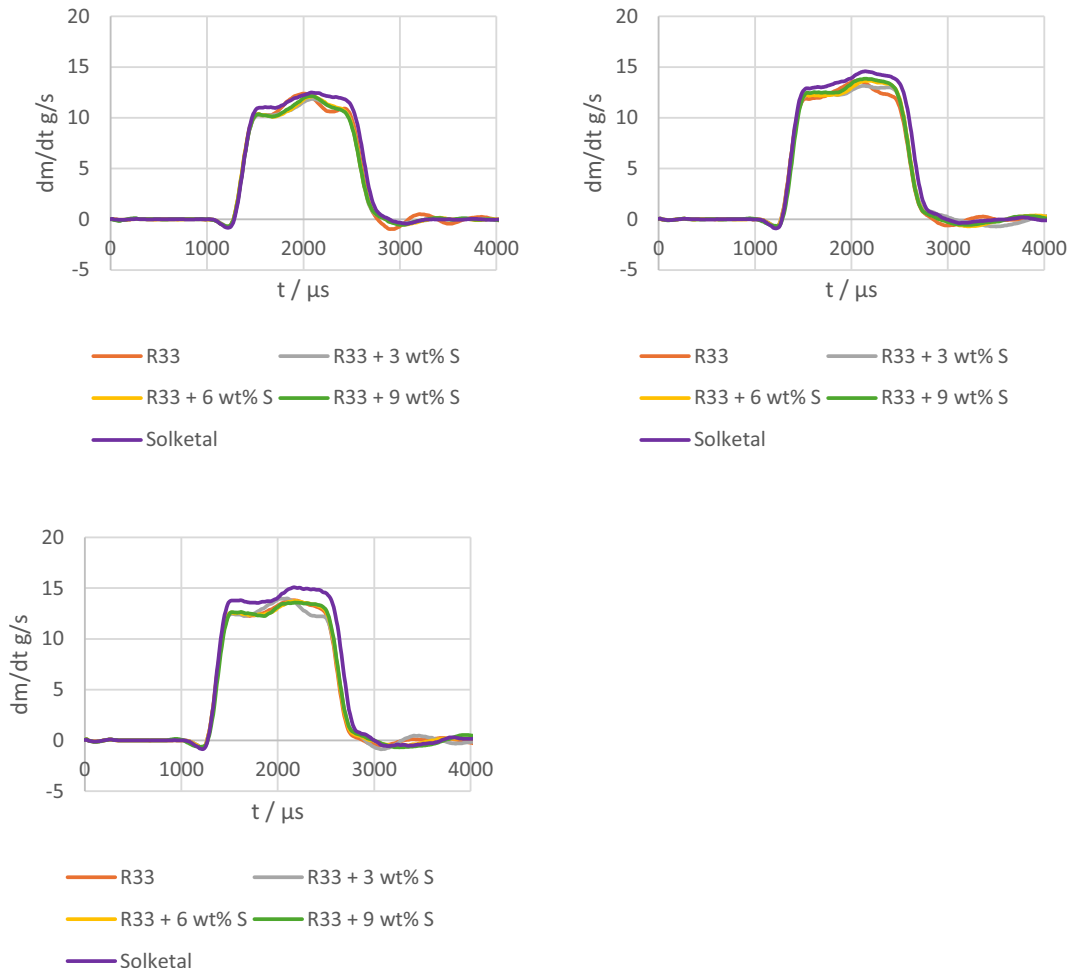

Fig. 5. Comparison of Diesel R33 pure and blended with solketal with pure solketal at different fuel temperatures (Top left: −20 °C, top right: 25 °C and bottom left: 90 °C). During the measurement, the ambient pressure (60 bar), the injection pressure (1500 bar) and the energizing time (1500 µs) were kept constant.

Table 3
Illustration of the densities of the fuels examined: Solketal, Diesel R33 and Diesel R33 containing solketal.

	R33	R33 + 3 wt % S	R33 + 6 wt % S	R33 + 9 wt % S	Solketal
Density [kg/m^3]	822.2	829.8	836.7	843.5	1063

the size increases continuously. This behavior is the result of the transition from the liquid to the gas phase. In order to establish comparability, the maximum penetration depth achieved in the liquid gas phase was defined analogously to Section 3.1. In contrast, the penetration depth at 2400 µs was selected due to the increase in this value during the investigation. The achieved penetration depth is significantly greater in the gas phase. The trends in the cone angle reach a maximum, then level off and reach an approximately constant value. In the liquid phase, the decrease is more distinct than in the gas phase (~50 % more). Here, the quasi-stationary value that occurs later in the injection is used. In general, it can be said that the quasi-stationary state of the cone angle does not change when the physical conditions change. The same applies to the comparison between the gas and liquid phases, which move within the same range depending on the phase (see Table 5).

In the liquid phase, it can be seen that the fuel temperature has a minor influence, with the lowest penetration depth being achieved in cold conditions at −20 °C. 25 and 90 °C exhibit approximately the same length (0.8 % difference). In addition, the curve at 90 °C shows a small delay in the start of the propagation until a later start of injection. The tendency for the start of injection is also observed for the penetration depth in the gas phase, where the increases are comparatively similar to that in the liquid phase. The cone angles show that the tendency of the injection timing correlates with those of the penetration depths in the liquid phase. There is no significant difference in the proceeding measurement of the cone angle. Solketal therefore shows no deviations such as cavitation and exhibits fuel air mixture formation similar to that of established fuels.

For the injection pressure, in liquid phase, it can be seen that the absolute penetration depth remains the same, but the time at which the fuel spreads occur later with increasing pressure. It is also observable that the lower the injection pressure, the longer the injection takes. In the gas phase, however, the absolute penetration depth increases with increasing injection pressure compared to the liquid phase. This might indicate that the time of the transition from the liquid to the gas phase in terms of the penetration depth may not be influenced by the injection pressures. Theoretically, the time required to achieve the mixture necessary for complete vaporization depends on the injection pressure, as the propagation speed changes [39]. However, solketal appears to be more volatile than other fuel components. In addition, it achieves lower liquid penetration depths, which leads to difficulties in resolution. The phase transition appears to occur at the same penetration depth, which is due to the same thermodynamic conditions at the three injection pressures. It is derived from the fact that the injection pressure has no influence on the local mixture ratio [39]. Considering the cone angle, the quasi-stationary state of the angle does not change. This correlates

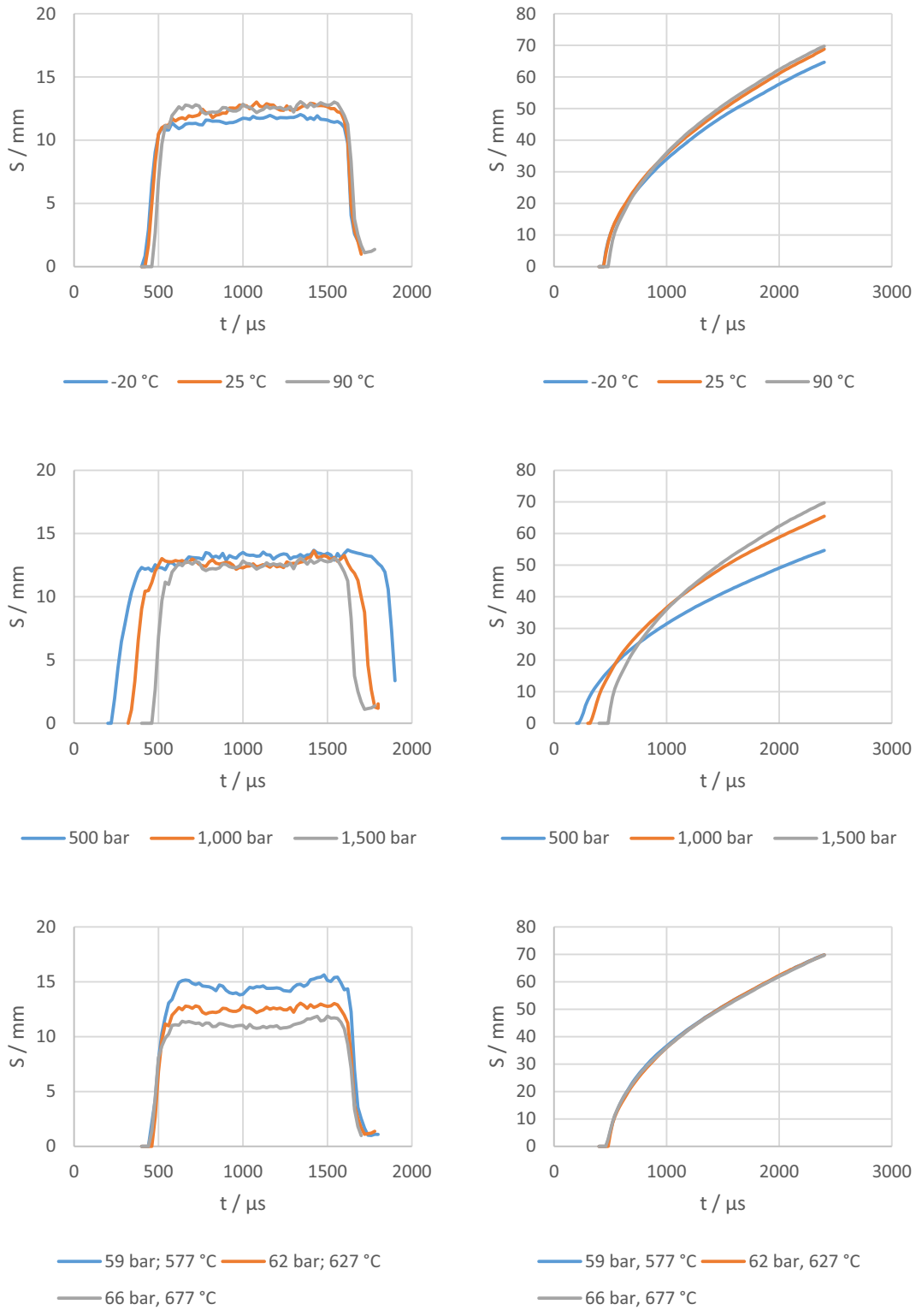

Fig. 6. Penetration depth progression of neat solketal with changes in fuel temperature, injection pressure and ambient conditions. The left side displays the liquid phase using Mie scattering, while the right side displays the gas phase using schlieren optics. The energizing time conducted 1500 µs with 0 % of oxygen content of the ambient gas.

with the penetration depths, which also exhibit the same maximum penetration depths in the liquid phase. In general, higher injection pressures should lead to stronger atomization [40]. However, the increase in injection pressure can result in a reduced [41] or increased [42] cone angle. Neither is detectable in liquid or gas phase. Furthermore, the cone angle shows the same tendency for the beginning of the spread of fuel spray. Only the length of the increase in the cone angle is different compared to the liquid phase, where the process was observed for a longer time. This lower slope is the result of the lower fuel velocity caused by the injection pressures.

The penetration depth of solketal varies when the ambient conditions change. There is a tendency for the depth of penetration to increase

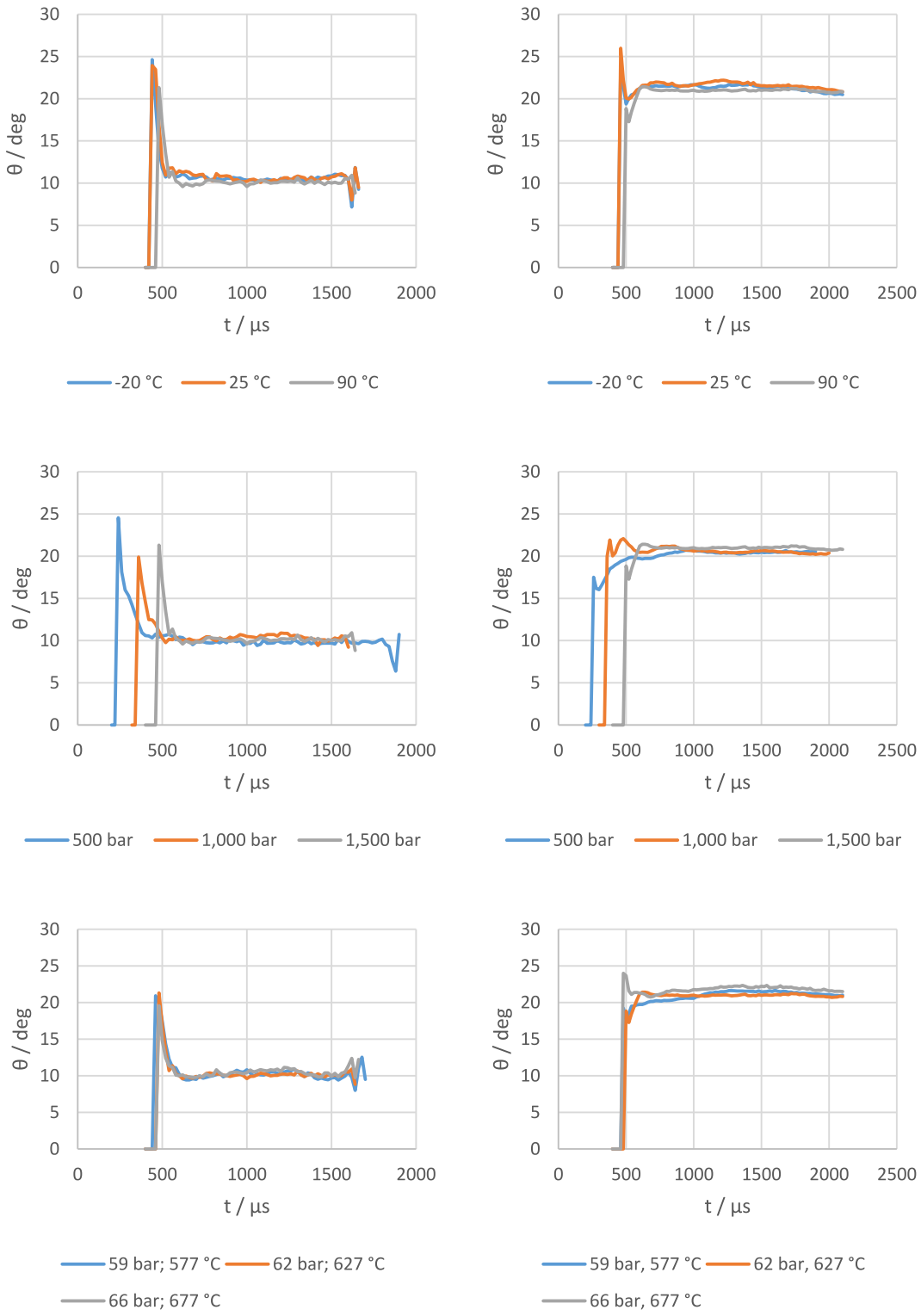

Fig. 7. Cone angle progression of neat solketal with changes in fuel temperature, injection pressure and ambient conditions. The left side displays the liquid phase using Mie scattering, while the right side displays the gas phase using schlieren optics. The energizing time conducted 1500 µs with 0 % of oxygen content of the ambient gas.

at lower ambient pressure and temperature. At higher temperatures and pressures, the solketal appears to transition from the liquid to the gas phase earlier. Furthermore, various models of the liquid penetration depth show a proportionality of $S \propto p_a^{-0.25}$ [43]. Therefore, an increase in ambient pressure and temperature results in a lower penetration depth of the liquid phase. In the gas phase, the penetration depth plots for different ambient conditions show approximately the same progress. This indicates that the variation of the ambient conditions might have an influence on the phase transition. In the liquid phase, no influence on the cone angle was observed, except the starting point of the increase of the cone angle. Regarding the start of the spread of the fuel spray, it is evident that the propagation starts earliest at 66 bar and 677 °C in the

Table 4
List of penetration depths and increases at different fuel temperatures, injection pressures and ambient conditions. The left side describes the liquid phase, which is defined by the maximum penetration depth achieved during the measurement. The right side describes the gas phase. Here, the penetration depths were compared with each other after 2400 µs.

	Liquid Phase			Gas phase	
Fuel temperature [°C]	Penetration depth [mm]	Increase [%]	Fuel temperature [°C]	Penetration depth [mm]	Increase [%]
−20	12.0	/	−20	64.7	/
25	13.0	7.7	25	68.8	6.0
90	13.1	0.8	90	69.8	1.4
Injection pressure [bar]	Penetration depth [mm]	Increase [%]	Injection pressure [bar]	Penetration depth [mm]	Increase [%]
500	13.7	/	500	54.7	/
1000	13.6	−0.7	1000	65.5	6.5
1500	13.1	−3.7	1500	69.8	6.2
Ambient conditions	Penetration depth [mm]	Increase [%]	Ambient conditions	Penetration depth [mm]	Increase [%]
59 bar, 577 °C	15.6	/	59 bar, 577 °C	69.8	/
62 bar, 627 °C	13.1	−16.0	62 bar, 627 °C	69.8	0
66 bar, 677 °C	11.9	−9.2	66 bar, 677 °C	69.6	−0.3

Table 5
List of cone angles and increases at different fuel temperatures, injection pressures and ambient conditions. The left side describes the liquid phase and the right side the gas phase. To ensure a comparison of the cone angle, the maxima were compared.

Liquid Phase		Gas phase		
Fuel temperature [°C]	Cone angle [deg]	Fuel temperature [°C]	Cone angle [deg]	Increase between l and g phase [%]
−20	10.5	−20	21.1	49.7/
25	10.6	25	21.4	49.1/
90	10.1	90	20.4	50.5/
Injection pressure [bar]	Cone angle [deg]	Injection pressure [bar]	Cone angle [deg]	Increase between l and g phase [%]
500	9.9	500	20.4	51.5/
1000	10.3	1000	20.4	50.5/
1500	10.1	1500	20.4	50.5/
Ambient conditions	Cone angle [deg]	Ambient conditions	Cone angle [deg]	Increase between l and g phase [%]
59 bar, 577 °C	10.1	59 bar, 577 °C	21.1	52.1/
62 bar, 627 °C	10.1	62 bar, 627 °C	20.4	50.5/
66 bar, 677 °C	10.5	66 bar, 677 °C	21.7	48.4/

gas phase. The two plots at the lower ambient conditions are similar. However, the point at which the cone angle increases occur a little later at higher ambient conditions. In general, ambient temperature and pressure have an influence on the air entrainment and thus on the atomization [44]. However, studies have demonstrated that there is no significant difference in air entrainment when the Schlieren penetration depth and the cone angle are nearly identical [45]. On the one hand, it is crucial for air entrainment that the density of the ambient conditions at the operating points investigated remains constant. Atomization, on the other hand, is primarily determined by fuel properties and injection pressure, which do not change.

3.3. Spray investigation of Diesel R33 containing solketal

After evaluating solketal as a pure component, the influence on Diesel R33 is examined. Fig. 8 shows the fuel temperature at −20 °C and the variation of the ambient conditions. The supporting information shows the other conditions as well as one exemplary cone angle plot. The cone angles remained roughly in the same size range and for the most part showed the same behavior. In terms of penetration depth, generally, it can be seen that Diesel R33 has a greater depth of penetration at elevated ambient conditions than the reference diesel fuel in the liquid phase. At 59 bar and 577 °C, the progressions are approximately the same. The depth of penetration range in which all fuels fit also decreases as the ambient conditions increase. This is a further indication of the earlier transition to the gas phase for all fuel blends. The blends show a greater penetration depth than pure solketal. This should be due to the fact that solketal enters the gas phase earlier compared to other diesel fuels due to its comparatively low boiling range (solketal: 190 °C [46] and diesel fuel boiling range: 177–343 °C [47]. This is supported by the Diesel R33 mixtures by varying the ambient conditions, which also show a lower penetration depth with increasing solketal content. Furthermore, as a pure component, solketal has a higher density and surface tension [38], which can have the effect of reducing the atomization [48]. However, the cold temperature behavior seems remarkable since the greatest difference is seen at the fuel temperature of −20 °C (34 % less penetration depth compared to Diesel R33). It is observable in both phases. Solketal shows the lowest penetration depth there, due to the fact that the greatest impact of viscosity, density and surface tension is here. Moreover, the injection rate decreases slightly more compared to other fuel components (see Section 3.1). In general, the injection rate reacts to the solketal content, which therefore indicates an influence on the hydraulics of the injector. This influences the initial momentum and thus the air entrainment. By contrast, the HVO-containing fuels have good low-temperature properties [49]. The influence of solketal on the spray properties in Diesel R33 blends in the gas phase is basically equivalent (see Fig. 9). However, the comparison of the fuels with each other in terms of the penetration depths of the variation in the ambient conditions shows the following (see supporting information). It can be seen that for all conditions, Diesel R33 has the greatest penetration depth, followed by the reference diesel and solketal, which penetrate approximately the same distance. The Diesel R33 blends with solketal tend to show similar penetration depths. However, a trend with a decrease of penetration depth with higher solketal content is observable. It can be concluded that solketal affects the spray properties of Diesel R33. However, these are not affected to such an extent that they become not useable as drop-in fuel.

4. Conclusion and outlook

In general, solketal has been shown to be suitable for drop-in use in terms of spray formation as a pure substance and in a multi-component system, based on diesel engine conditions. However, it has been shown that solketal has an influence on the mass flow, depth of penetration and the cone angle.

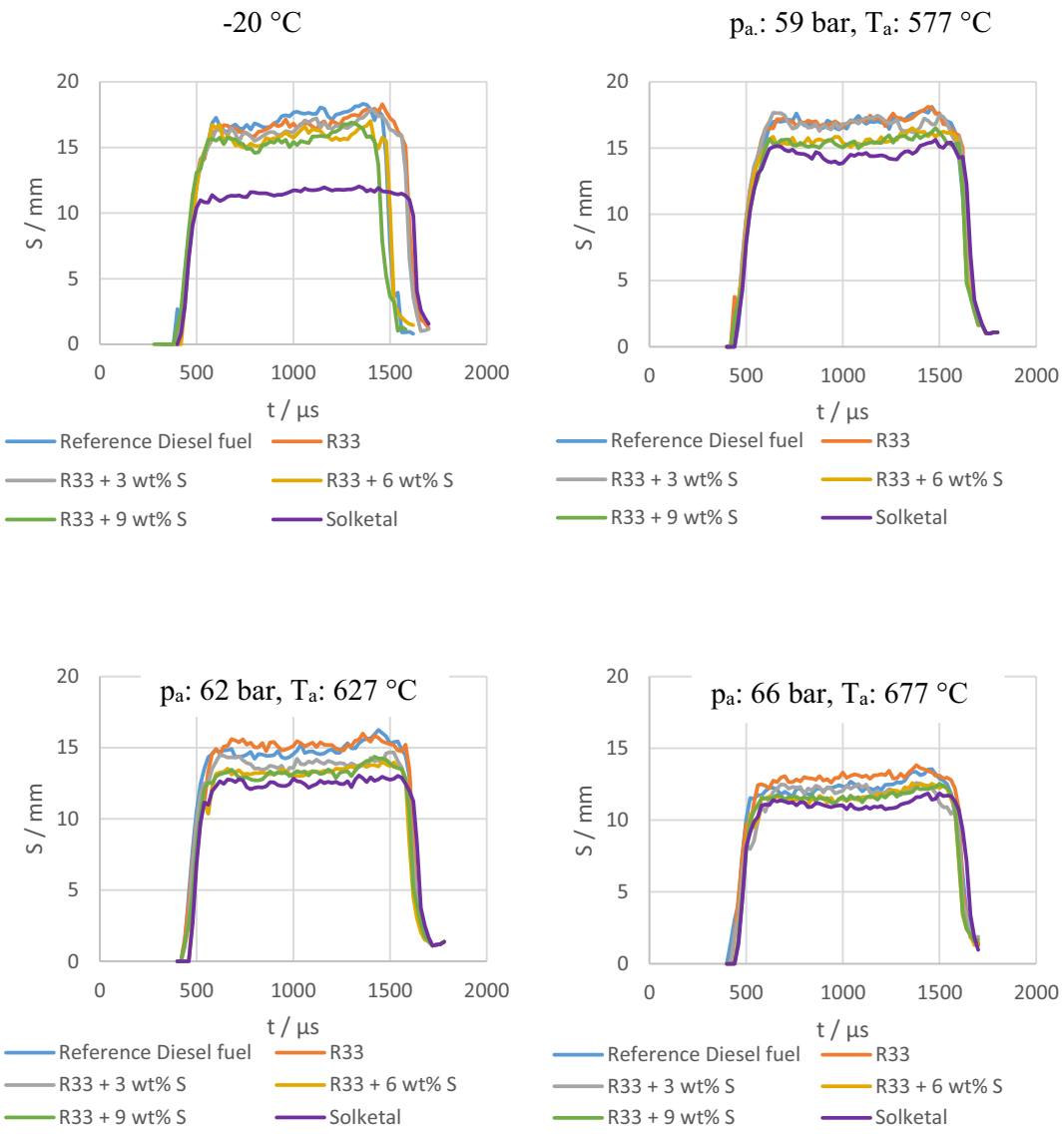

Fig. 8. Comparison of penetration depths in the liquid phase via Mie scattering between neat solketal, Diesel R33 with and without solketal, and a reference diesel fuel. This fig. Represents the cold fuel temperature of −20 °C and the change in ambient conditions. The energizing time conducted 1500 µs with 0 % of oxygen content of the ambient gas.

With regard to the mass flow when varying the fuel temperature and the injection pressure, it is evident that solketal follows the expected behavior that an increase in these parameters also results in an increase in mass flow. Nevertheless, it can be seen that solketal, due to its greater density and viscosity, tend to have an increasing influence on the mass flow of the diesel fuel blend. The same observation occurs when the penetration depth and cone angle of solketal are examined. The results are as expected when the fuel temperature, injection pressure and ambient conditions change. However, the influence of solketal on Diesel R33 and the comparison with the pure component show that solketal tends to cause lower penetration depths. One factor here is the increased density and viscosity, as well as the surface tension, which makes atomization more challenging. The behavior at a fuel temperature of −20 °C is particularly striking, where the increased viscosity compared to multicomponent systems leads to a significantly lower depth of penetration. This becomes apparent when compared with Diesel R33, where solketal shows a reduction of 34 %. It is also noticeable that solketal tends to be present in the gas phase earlier due to its comparatively lower boiling point. No systematic influence of solketal on the cone angle was observed. However, this study demonstrates that solketal is suitable for use in diesel injection systems in terms of its spray formation. This opens up the possibility of adding more non-fossil fuels, which could lead to a reduction in greenhouse gases.

Since the spray behavior of solketal has been described and analyzed, the next step is to examine the ignition behavior of these fuels. The chemical structure and physical properties of solketal should be discussed. In addition, a deeper understanding of the influences and interactions of individual components with respect to each other should be acquired. The ignition delay, soot luminescence and OH radical formation should be addressed in order to obtain initial indications of soot formation. Furthermore, engine tests must be carried out, as these tests in the injection chamber only represent part of the combustion process.

CRediT authorship contribution statement

Julian Türck: Writing – original draft, Visualization, Investigation, Data curation, Conceptualization. **Sebastian Riess:** Writing – review & editing, Supervision, Methodology, Investigation, Data curation. **Lukas Strauß:** Writing – review & editing, Investigation, Data curation. **Fabian Schmitt:** Writing – review & editing, Supervision, Conceptualization.

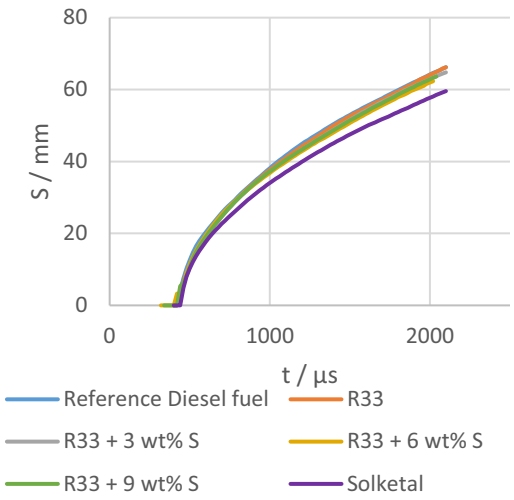

Fig. 9. Progression of penetration depth at a fuel temperature of −20 °C in the gas phase. The figure displays the comparison between neat solketal, Diesel R33 with and without solketal, and a reference diesel fuel. The energizing time conducted 1500 µs with 0 % of oxygen content of the ambient gas.

Ralf Türck: Writing – review & editing, Project administration, Funding acquisition. **Wolfgang Ruck:** Writing – review & editing, Project administration. **Michael Wensing:** Writing – review & editing, Project administration, Formal analysis, Conceptualization. **Jürgen Krahl:** Writing – review & editing, Visualization, Supervision, Project administration, Funding acquisition.

Declaration of competing interest

The authors declare that they have no known competing financial interests or personal relationships that could have appeared to influence the work reported in this paper.

Data availability

Data will be made available on request.

References

[1] K. Götz, B. Fey, A. Singer, J. Krahl, J. Bünger, M. Knorr, O. Schröder, Exhaust Gas Emissions and Engine Oil Interactions from a New Biobased Fuel Named Diesel R33, SAE Technical Paper, 2016.
[2] E.C.f. Standardization, Standard EN 590. Automotive Fuels – Diesel – Requirements and Test Methods, 2025.
[3] A. Dimitriadis, I. Natsios, A. Dimaratos, D. Katsaounis, Z. Samaras, S. Bezergianni, K. Lehto, Evaluation of a hydrotreated vegetable oil (HVO) and effects on emissions of a passenger car diesel engine, Front. Mech. Eng. 4 (2018) 7.
[4] K. Sorate, P. Bhale, Impact of Biodiesel on Fuel System Materials Durability, 2013.
[5] G. Micallef, Elastomer selection for bio-fuel requires a systems approach, Seal. Technol. 2009 (2009) 7–10.
[6] W. Stone, G. Bessee, C. Stanfel, Diesel fuel/water separation test methods—where we are and where we are going, SAE Int. J. Fuels Lubr. 2 (2009) 317–323.
[7] V. Betgeri, O.P. Bhardwaj, S. Pischinger, Investigation of the drop-in capabilities of a renewable 1-Octanol based E-fuel for heavy-duty engine applications, Energy 282 (2023) 128811.
[8] J. Hunicz, J. Matijošius, A. Rimkus, A. Kilikevičius, P. Kordos, M. Mikulski, Efficient hydrotreated vegetable oil combustion under partially premixed conditions with heavy exhaust gas recirculation, Fuel 268 (2020) 117350.
[9] H. Ulrich, B. Lehnert, D. Guénot, K. Svendsen, O. Lundh, M. Wensing, E. Berrocal, L. Zigan, Effects of liquid properties on atomization and spray characteristics studied by planar two-photon fluorescence, Phys. Fluids 34 (2022).
[10] M.R. Monteiro, C.L. Kugelmeier, R.S. Pinheiro, M.O. Batalha, A. da Silva César, Glycerol from biodiesel production: technological paths for sustainability, Renew. Sust. Energ. Rev. 88 (2018) 109–122.
[11] J. Kaur, A.K. Sarma, M.K. Jha, P. Gera, Valorisation of crude glycerol to value-added products: Perspectives of process technology, economics and environmental issues, Biotechnol. Rep. 27 (2020) e00487.
[12] N.I.W. Azelee, A.N.M. Ramli, N.A. Manas, N. Salamun, R.C. Man, H. El Enshasy, Glycerol in food, cosmetics and pharmaceutical industries: basics and new applications, Int. J. Sci. Technol. Res. 8 (2019) 553–558.
[13] S.A. Steinmetz, J.S. Herrington, C.K. Winterrowd, W.L. Roberts, J.O. Wendt, W. P. Linak, Crude glycerol combustion: particulate, acrolein, and other volatile organic emissions, Proc. Combust. Inst. 34 (2013) 2749–2757.
[14] M. Stelmachowski, Utilization of glycerol, a by-product of the transestrification process of vegetable oils: a review, Ecol. Chem. Eng. 18 (S) (2011) 9–30.
[15] R. Nicol, K. Marchand, W. Lubitz, Bioconversion of crude glycerol by fungi, Appl. Microbiol. Biotechnol. 93 (2012) 1865–1875.
[16] M.R. Nanda, Y. Zhang, Z. Yuan, W. Qin, H.S. Ghaziaskar, C.C. Xu, Catalytic conversion of glycerol for sustainable production of solketal as a fuel additive: a review, Renew. Sust. Energ. Rev. 56 (2016) 1022–1031.
[17] W. Park, S. Park, R.D. Reitz, E. Kurtz, The effect of oxygenated fuel properties on diesel spray combustion and soot formation, Combust. Flame 180 (2017) 276–283.
[18] J. Türck, F. Schmitt, L. Anthofer, A. Lichtinger, R. Türck, W. Ruck, J. Krahl, Oxidation Kinetics of Neat Methyl Oleate and as a Blend with Solketal, Energies 16 (2023) 3253.
[19] J. Türck, F. Schmitt, L. Anthofer, R. Türck, W. Ruck, J. Krahl, Extension of biodiesel aging mechanism–the role and influence of Methyl Oleate and the contribution of Alcohols through the use of Solketal, ChemSusChem 16 (2023) e202300263.
[20] F. Kerkel, D. Brock, D. Touraud, W. Kunz, Stabilisation of biofuels with hydrophilic, natural antioxidants solubilised by glycerol derivatives, Fuel 284 (2021) 119055.
[21] E. Alptekin, M. Canakci, Performance and emission characteristics of solketal-gasoline fuel blend in a vehicle with spark ignition engine, Appl. Therm. Eng. 124 (2017) 504–509.
[22] J. Türck, A. Singer, A. Lichtinger, M. Almaddad, R. Türck, M. Jakob, T. Garbe, W. Ruck, J. Krahl, Solketal as a renewable fuel component in ternary blends with biodiesel and diesel fuel or HVO and the impact on physical and chemical properties, Fuel 310 (2022) 122463.
[23] P. Sharma, M.P. Le, A. Chhillar, Z. Said, B. Deepanraj, D.N. Cao, S.A. Bandh, A. T. Hoang, Using response surface methodology approach for optimizing performance and emission parameters of diesel engine powered with ternary blend of Solketal-biodiesel-diesel, Sustain Energy Technol Assess 52 (2022) 102343.
[24] C.-Y. Lin, S.-M. Tsai, Emission characteristics of a diesel engine fueled with nanoemulsions of continuous diesel dispersed with solketal droplets, J. Environ. Sci. Health A 55 (2020) 224–229.
[25] C. Yao, P. Geng, Z. Yin, J. Hu, D. Chen, Y. Ju, Impacts of nozzle geometry on spray combustion of high pressure common rail injectors in a constant volume combustion chamber, Fuel 179 (2016) 235–245.
[26] D.D. Wickman, P.K. Senecal, R.D. Reitz, Diesel engine combustion chamber geometry optimization using genetic algorithms and multi-dimensional spray and combustion modeling, SAE Trans. (2001) 487–507.
[27] S.H. Park, S.H. Yoon, C.S. Lee, Effects of multiple-injection strategies on overall spray behavior, combustion, and emissions reduction characteristics of biodiesel fuel, Appl. Energy 88 (2011) 88–98.
[28] Z. Shi, C.-f. Lee, H. Wu, H. Li, Y. Wu, L. Zhang, Y. Bo, F. Liu, Effect of injection pressure on the impinging spray and ignition characteristics of the heavy-duty diesel engine under low-temperature conditions, Appl. Energy 262 (2020) 114552.
[29] U. Sonawane, A.K. Agarwal, Comparative spray atomization and evaporation characteristics of dimethyl ether and mineral diesel, J. Energy Resour. Technol. 145 (2023).
[30] L. Chen, R. Stone, Measurement of enthalpies of vaporization of isooctane and ethanol blends and their effects on PM emissions from a GDI engine, Energy Fuel 25 (2011) 1254–1259.
[31] A. Vaudrey, Thermodynamics of indirect water injection in internal combustion engines: analysis of the fresh mixture cooling effect, Int. J. Engine Res. 20 (2019) 527–539.
[32] R.K. Pandey, A. Rehman, R. Sarviya, Impact of alternative fuel properties on fuel spray behavior and atomization, Renew. Sust. Energ. Rev. 16 (2012) 1762–1778.
[33] J. Dernotte, C. Hespel, F. Foucher, S. Houille, C. Mounaïm-Rousselle, Influence of physical fuel properties on the injection rate in a Diesel injector, Fuel 96 (2012) 153–160.
[34] M. Das, M. Sarkar, A. Datta, A.K. Santra, Study on viscosity and surface tension properties of biodiesel-diesel blends and their effects on spray parameters for CI engines, Fuel 220 (2018) 769–779.
[35] The fuel rate indicator: a new measuring instrument for display of the characteristics of individual injection, W, Bosch, 1967, pp. 641–662.
[36] S. Busch, P.C. Miles, Parametric study of injection rates with solenoid injectors in an injection quantity and rate measuring device, J. Eng. Gas Turbines Power 137 (10) (2015) 101503.
[37] S. Riess, L. Weiss, A. Peter, J. Rezaei, M. Wensing, Air entrainment and mixture distribution in Diesel sprays investigated by optical measurement techniques, International Journal of Engine Research 19 (1) (2018) 120–133.
[38] Glaconchemie. 2025.
[39] K. Nishida, Y. Ogata, Evaporation and mixture formation characteristics of diesel spray under various nozzle hole size and injection pressure condition employing similar injection rate profile, Int. Commun. Heat Mass Transfer 123 (2021) 105184.
[40] R. Palani, N. Nallusamy, K. Pitchandi, Spray characteristics of diesel and derivatives in direct injection diesel engines with varying injection pressures, J. Mech. Sci. Technol. 29 (2015) 4465–4471.
[41] M. Hawi, H. Kosaka, S. Sato, T. Nagasawa, A. Elwardany, M. Ahmed, Effect of injection pressure and ambient density on spray characteristics of diesel and biodiesel surrogate fuels, Fuel 254 (2019) 115674.
[42] T.-M. Jia, Y.-S. Yu, G.-X. Li, Experimental investigation of effects of super high injection pressure on diesel spray and induced shock waves characteristics, Exp. Thermal Fluid Sci. 85 (2017) 399–408.

[43] J. Desantes, R. Payri, F. Salvador, V. Soare, Study of the Influence of Geometrical and Injection Parameters on Diesel Sprays Characteristics in Isothermal Conditions, SAE Technical Paper, 2005.
[44] A.H. Lefebvre, V.G. McDonell, Atomization and Sprays, CRC Press, 2017.
[45] S. Riess, J. Rezaei, L. Weiss, A. Peter, M. Wensing, Phase change in fuel sprays at diesel engine ambient conditions: modeling and experimental validation, J. Supercrit. Fluids 173 (2021) 105224.
[46] I. Corrêa, R.P. Faria, A.E. Rodrigues, Continuous valorization of glycerol into solketal: recent advances on catalysts, processes, and industrial perspectives, Sustain. Chem. 2 (2021) 286–324.
[47] C.S. Hsu, Diesel fuel analysis, in: Encyclopedia of Anal. Chem., 2000, pp. 6613–6622.
[48] J. Shin, D. Kim, J. Seo, S. Park, Effects of the physical properties of fuel on spray characteristics from a gas turbine nozzle, Energy 205 (2020) 118090.
[49] T. Hartikka, M. Kuronen, U. Kiiski, Technical Performance of HVO (Hydrotreated Vegetable Oil) in Diesel Engines, SAE Technical Paper, 2012.

Julian Türck is a German scientist specializing in research into sustainable fuels, particularly the use of solketal as a renewable fuel component. After completing his bachelor's degree in chemistry at the University of Heidelberg, he continued his academic career with a master's degree at the Technical University of Munich (TUM). After completing his master's degree, Julian Türck joined the research facility at Leuphana University Lüneburg as a Ph.D. student. There, he focused on investigating solketal and its application in various fuel blends, particularly in biodiesel and diesel. During his time at the university, he worked intensively on the chemical and physical properties of solketal and its influence on the aging processes of fuels. This research is of crucial importance as it helps to improve the stability and long-term quality of biodiesel and diesel, thereby contributing to the development of more sustainable and environmentally friendly fuels. In addition to his academic work, Julian Türck collaborates with Tecosol GmbH in Ochsenfurt. There, he investigates the practical applications of solketal in real fuel blends and contributes to the development of ternary fuel blends that combine biodiesel, diesel and hydrogenated vegetable oils (HVO). This work supports the industrialisation of sustainable fuels that are both powerful and environmentally friendly.